DOI 10.52209/2706-977X_2026_1_81 **IRSTI 81.09.03** **UDC 004.942**

Comparative Mechanical Performance of Cylindrical and Cuboid Pore Geometries in Additively Manufactured ABS Bone Scaffolds

Modi Yashwant Kumar*
Jaypee University of Engineering and Technology, Guna, India
*corresponding author

Abstract. Synthetic bone scaffold must possess a good balance of porosity and mechanical strength for success of the tissue engineering process. With availability of additive manufacturing (AM) technology, it is possible to fabricate porous scaffolds with customised porosity, pore shape and size; which was rather difficult for the traditional processes. This paper presents design, analysis and additive manufacturing of ABS porous bone scaffolds. It also compares mechanical behaviour of the porous scaffolds with different pore geometry. Initially, two CAD models with same porosity but different pore geometry were created in Solidworks®2016. Then, finite element analysis (FEA) of both the scaffolds was conducted in ANSYS® Workbench for von-Mises stress, elastic strain and total deformation by applying a compressive load of 500N. On comparing, stress-strain curve of scaffold with cylindrical channels found to be steeper than scaffold with cuboid channels. Moreover, Young's modulus of scaffold with cylindrical channels (2587 MPa) was found greater than the scaffold with cuboid channels (2512 MPa). Stress-strain curve obtained via physical testing of specimens also found to follow similar tends. This result leads to conclude that scaffolds with cylindrical channels can withstand more loads in comparison with scaffolds with cuboid channels for the same porosity.

Keywords: additive manufacturing; compressive strength; finite element analysis; porosity; porous bone scaffold; fuse deposition modelling.

Introduction

Additive Manufacturing (AM), originally introduced in 1980s with the name rapid prototyping, is an umbrella term for a host of manufacturing processes, which can fabricate physical part directly from a CAD model in additive manner [1]. ASTM International has classified AM technologies into seven major categories; namely, vat photo-polymerisation, material extrusion, binder jetting, material jetting, powder bed fusion, sheet lamination and directed energy deposition [2]. AM has been maturing day by day for more than past 35 years and today with increased technological knowhow and range of materials, it has become capable of producing even end-use functional components in metal, polymer and ceramics [3-5]. One of the key advantages of AM is the ability to produce complex shapes and geometries such as pre-designed lattice structures to reduce weight, that are very difficult or even impossible for other manufacturing processes [6-8]. To fabricate a part via AM process, initially, one need to have a CAD model in STL (**ST**ereo**L**ithography or Standard Triangulation Language) format, which is then converted into sliced model and finally one slice at a time is sent to the AM machine, where part gets fabricated in layer by layer manner [9, 10].

Bone tissue engineering (BTE) is one of the fastest growing technologies, which is capable of developing implantable bone substitutes for large sized bone defects that cannot heal on their own [11-12]. The success of BTE depends on a supporting structure known as scaffold. This scaffold is expected to possess adequate porosity so that new tissues can grow properly and nutrients can flow inside it without any obstruction [13]. Moreover, it should also possess adequate mechanical strength so that it can withstand the pressure exerted by the growing tissues (for *in vitro* applications) as well as skeletal pressure in case of *in vivo* applications [14-16]. In addition to existing auto and allograft procedures, surgeons have been trying synthetic bone grafts for past few years. Synthetic bone graft employs a porous scaffold to seed, proliferate and mature the stem cells. Traditional scaffold making methods such as salt leaching, freeze drying, electro spinning suffer by several limitations, like difficulty in creating customised porosity, pore size, shape etc. [17-18]. In recent years, AM has emerged as a promising alternative to traditional methods for fabricating such customised scaffolds for BTE applications. A synthetic scaffold must have a good balance of porosity and mechanical strength so that it can allow free flow of nutrients and oxygen through proliferating stem cells as well as withstand the pressure exerted by the sprouting cells. Customized porosity, pore size and shape in scaffold can be designed during CAD model development. The objective of this study is to evaluate and compare the mechanical properties of acrylonitrile butadiene styrene (ABS) porous scaffolds with different pore geometry but same porosity by simulating their behaviour under compressive loading via FEA and physical testing of the additively manufactured specimens.

2.Material and Methods

2.1 Material

Acrylonitrile butadiene styrene (ABS) is one of the biocompatible materials processed by different AM processes [19]. It is an impact resistant thermoplastic polymer of three different monomers. Polymerization of different monomers imparts excellent physical, mechanical, chemical and electrical properties to ABS. It has been employed for making of variety of items such as pipe, telephone bodies, kitchen appliances, automotive components, wheel cover, helmet, toys, show-pieces etc. for past several years [20]. In recent years, it has been used in medical field also. Apart from manufacturing respiratory, auto-injection and infusion devices, it has also been applied to print miniature prosthetic implants, such as middle ear prostheses [21-23]. However, ABS can be used in medical applications when supplied in certified medical-grade formulations. These grades comply with ISO 10993 and often meet USP Class VI requirements, including cytotoxicity, sensitization, and irritation testing. These grades are suitable for non-implantable components such as device housings and surgical instrument handles. Regulatory acceptance typically requires compliance with agencies, such as U.S. Food and Drug Administration or EU MDR guidelines, along with material traceability and risk assessment. Standard ABS is generally not recommended for long-term implantable applications due to limited long-term bio-stability and potential additive leaching.

2.2 Methodology

Methodology adopted to conduct this study is presented in Figure 1. Initially, a suitable specimen shape and size was chosen for ABS material. The dimensions of the specimen were chosen according to ISO-604 standard. Then, CAD models with two different pore geometries were created with almost same porosities by hit and trial method. Then the CAD model was imported into ANSYS® Workbench to perform static structural analysis and compare von-Mises stress, elastic strain and total deformation using finite element method. After that, porous specimens were additively manufactured via fused deposition modelling (FDM) technology. Finally, results obtained via FEA and physical test were compared for both the pore geometries.

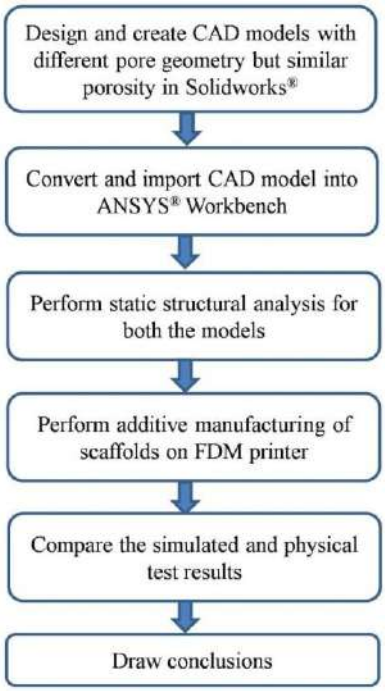

Fig. 1. - Methodology

2.3 CAD Modelling

A cuboid shaped specimen (25.4 mm × 12.7 mm × 12.7 mm), according to ISO 604 standard for compression testing was chosen for this study [24]. Two different CAD models of porous scaffolds were prepared with cuboid and cylindrical shaped pore channels using Solidworks®2016 software. Initially, several designs were prepared with slightly different sized channels to obtain the equal porosity. Initial designs were investigated with increasing number of channels (from 1, 2, 4, 8, 9 and 18) in three mutually perpendicular directions. Figures 2(a) and 2(b) show the CAD model of the porous scaffolds with cuboid and cylindrical channels.

Table 1. Specifications of CAD models of porous scaffolds

Characteristics	Cuboid channel	Cylindrical Channel
CAD model dimensions (mm) (L×B×H)	25.4 x 12.7 x 12.7	25.4 x 12.7 x 12.7
Cross section of channel (mm)	0.73 x 0.73	Φ 0.83
No. of channels along x,y and z-axis	18 x 9 x 9	18 x 9 x 9
Vol. of solid CAD model (mm^3)	4096.77	4096.77
Volume of porous CAD model (mm^3)	1941.97	1936.22
Porosity (%)	52.60	52.74

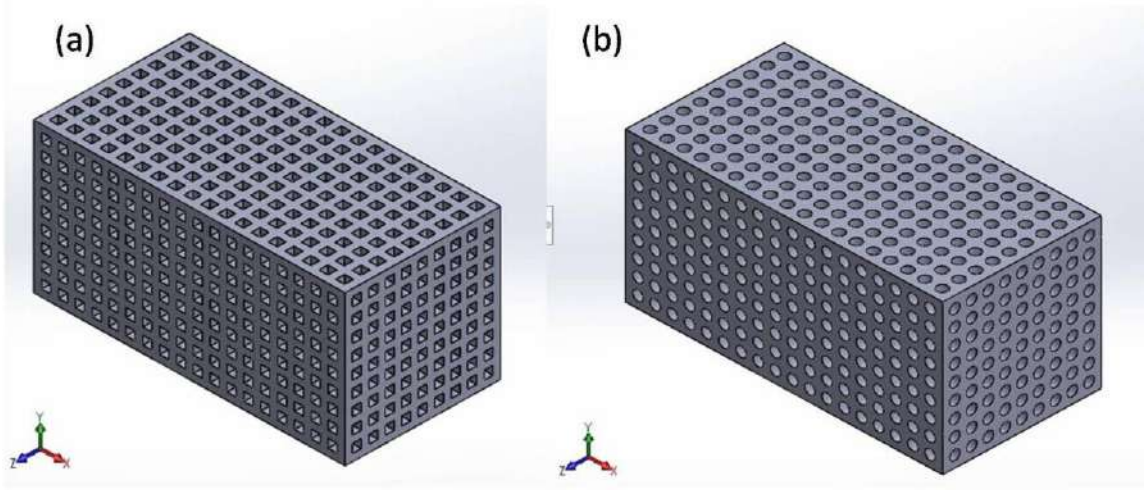

Fig. 2. - CAD model of porous scaffolds with (a) cuboid channels, (b) cylindrical channels

2.4 Finite Element Analysis

The behaviour of both the porous scaffold models under compressive loading has been simulated via finite element analysis using ANSYS® Workbench. The material properties of ABS plastic were used from the software itself (Poisson ratio = 0.35, Young's modulus = 2000 MPa). Initially, the model from Solidworks®2016 was imported in ANSYS® Workbench. For applying boundary conditions, one side (square face i.e. 12.7 mmx 12.7 mm) of the scaffold model was fixed and compressive load of 500 N was applied on other side of the scaffold. The load was applied along the length of model. The model was compressed at about 5% of its height and 1s time period at an increment of 0.01s was set. Then, static structural analysis under compression loading was performed on both CAD models. The results for von-Mises stress, elastic strain and total deformation were recorded. Simulated results were rendered in different colours to indicate the safety level of the models. The values of equivalent stress and strain were recorded to plot the stress-strain curve and calculate the Young's modulus for both the structures.

2.5 Additive Manufacturing

Porous specimens used in this study were printed using FDM process. In FDM process, a solid wire filament is passed through a heated extruder head, wherein it gets melted, extruded and finally deposited onto a substrate in layer by layer manner [25]. The extruder head is moved in xy-plane according to data obtained from the sliced model. Data of one slice is sent at a time to printer, which results in one layer. The substrate moves down by one layer thickness after printing each layer. Printing continues until full part is printed. Pratham 6.0, an FDM printer, shown in Figure 3(a), has been used to print the porous specimens. It is a heavy duty, industrial grade printer with a build volume of 600 mm x 600 mm x 600 mm. The specimens were printed on the following parameters, layer thickness: 0.2 mm and printing speed: 20 mm/sec. Three specimens of each type were printed. Photographs of the printed specimens are shown in Figure 3(b) and 3(c).

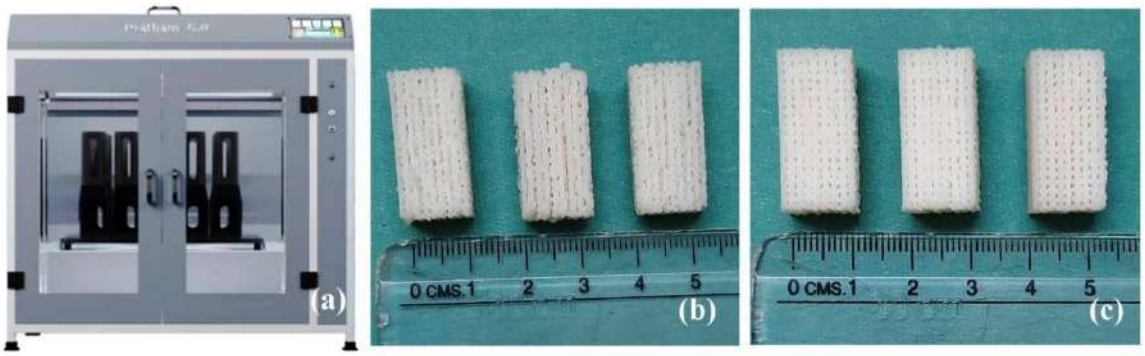

Fig. 3. - Photograps of a) FDM printer Pratham 6.0, b) scaffolds with cylindrical channels, c) scaffolds with cuboid channels

2.6 Testing of Compressive Strength

Compressive strength of printed porous specimens was tested on Tinius Olsen H5KL, a computerized compression testing machine with 5 kN load-cell and a cross-head loading rate of 2 mm per minute.

3. Result and Discussions

The simulated results for both the scaffold structures i.e. cuboid and cylindrical channels were obtained using ANSYS® Workbench. The rendered images with colour coded scale of both the structures for von-Mises stress, elastic strain and total deformation are shown in Figures 4, 5 and 6 respectively. In all the cases, load is applied on the top surface and bottom surface is fixed. The area where maximum and minimum stress and strain developed is shown in Figures 4 and 5 respectively.

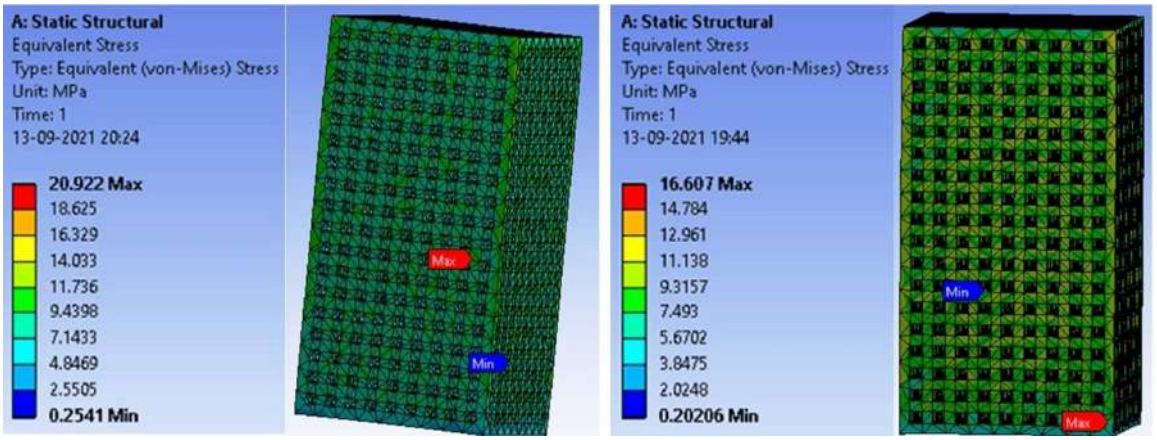

Fig. 4. - ANSYS results for von Mises stress of scaffolds with (a) cylindrical channels (b) cuboid channels

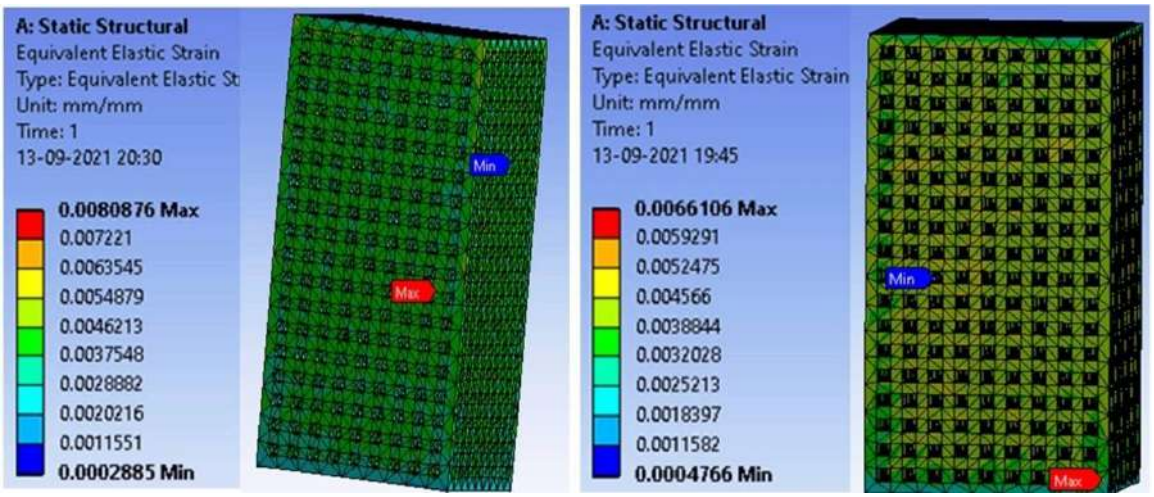

Fig. 5. - ANSYS results for equivalent elastic strain of scaffolds with (a) cylindrical channels (b) cuboid channels

Similarly, the amount of deformation can be seen with the help of rendered image and corresponding scale in Figure 6. Maximum deformation occurs at the face where compressive load is applied; which gradually decreases towards the fixed end and becomes the minimum at the fixed surface.

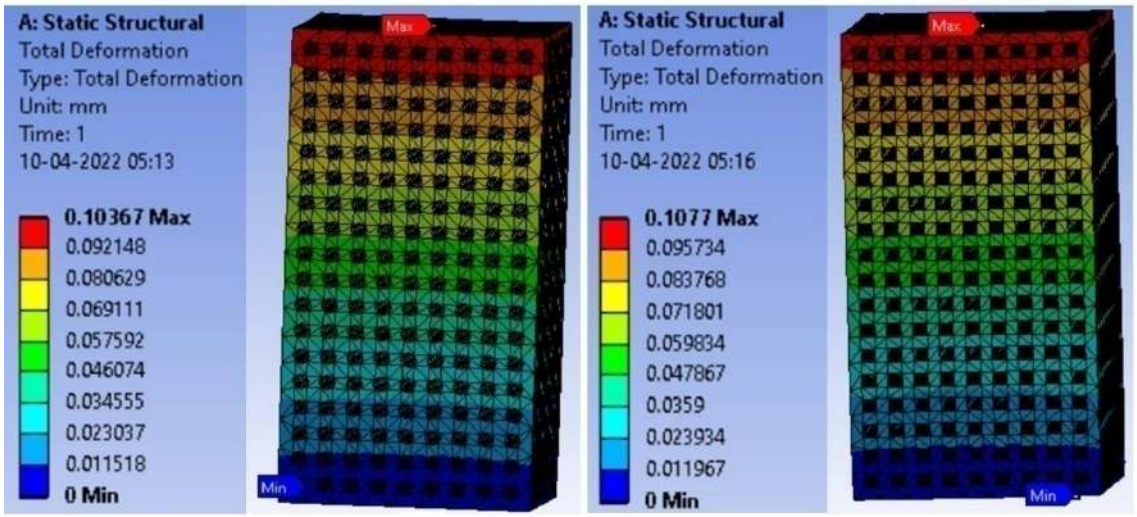

Fig. 6. - ANSYS results for total deformation of scaffolds with (a) cylindrical channels (b) cuboid channels

In Figure 7, stress-strain diagram obtained from linear static simulation for both the structures is shown. It can be seen that stress-strain curve of scaffold with cylindrical channels is steeper than the cuboid channels. This indicates that more force is required to compress the cylindrical channels than cuboid channels. The cylindrical channel consistently exhibits higher stress values at the same strain levels, demonstrating superior structural stiffness. From the slope of the curves, the effective elastic modulus of the cylindrical channel is approximately 25–30% higher than that of the cuboid channel. The cuboid channels consist of sharp edges, where stress concentration occurs that is responsible for lower elastic modulus. Therefore, it can be concluded that structure with cylindrical channels offers better elastic modulus and stiffness in comparison with cuboid channels.

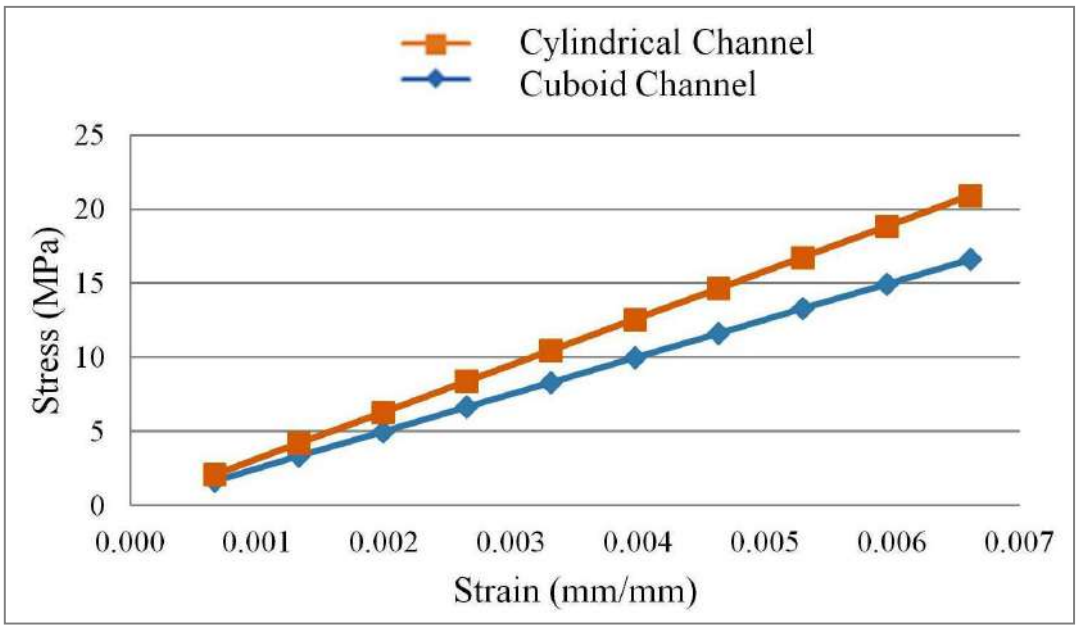

Fig. 7. - Stress-Strain curve for scaffolds with cylindrical and cuboid channels via FEA

Figure 8, presents a comparison of Young's modulus of scaffolds with both the structures. Young's modulus of scaffold with cylindrical channels is 2587 MPa, which is greater than the scaffold with cuboid channels (2512 MPa). This is because the strut region of the cylindrical channels is larger than the cuboid channels and offers more resistance. Moreover, sharp edges present in cuboid structure also make it slightly weaker. There is a difference in total deformation

of both the structures as well, as can be seen from the Figure 9. For cylindrical structure, it is 0.1036 mm; whereas for cuboid structure, it is 0.1077 mm. This also indicates that cylindrical structure possesses better compressive strength.

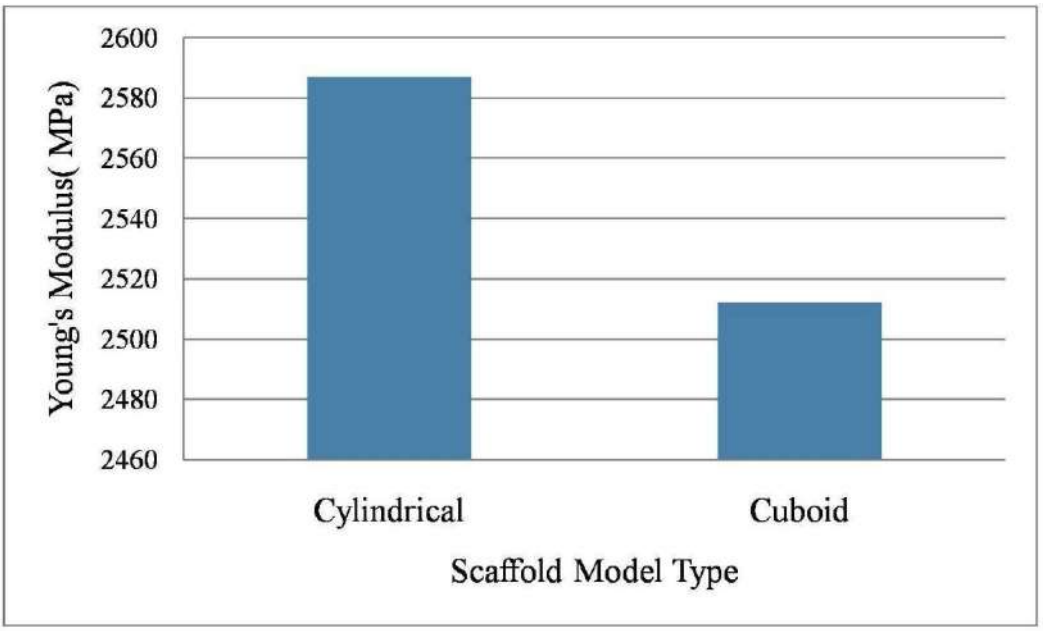

Fig. 8. - Young's modulus of scaffolds with cylindrical and cuboid channels

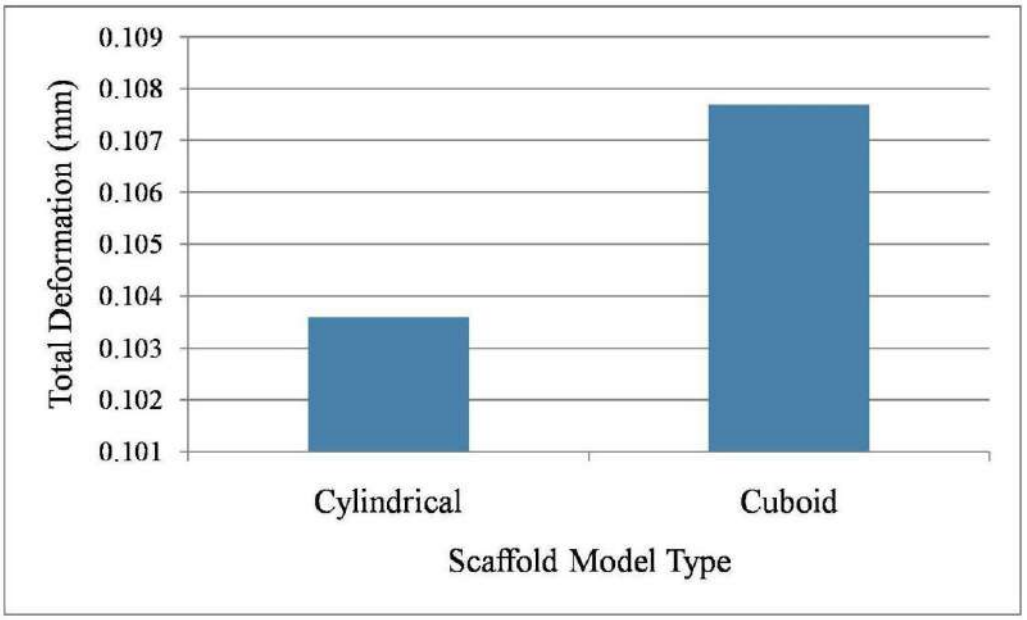

Fig. 9. - Total deformation of scaffolds with cylindrical and cuboid channels

The stress-strain curves obtained via compressive testing of physical specimens are shown in the Figure 10. It is clear from the Figure that scaffolds with cylindrical channels exhibit better mechanical performance in comparison with scaffold with cuboid channels.

On comparing Figure 7 and Figure 10, it can be observed that physical testing confirms results of FEA to some extent. The simulated and actual stress-strain curves show similar trend in elastic region. However, slight difference in stress and strain values in simulated and actual results may be due to the fact that Figure 7 represents an ideal linear static simulation, where the material and geometry are assumed to be perfectly elastic and free from imperfections. In contrast, Figure 10 is based on experimental results, where factors such as machine compliance, specimen alignment, surface contact effects, and minor geometric imperfections slightly reduce the initial stiffness, causing small deviations from perfect linearity. Moreover, slight variation in structural details between CAD model and actual fabricated specimens may also be responsible for introducing slight variation in results.

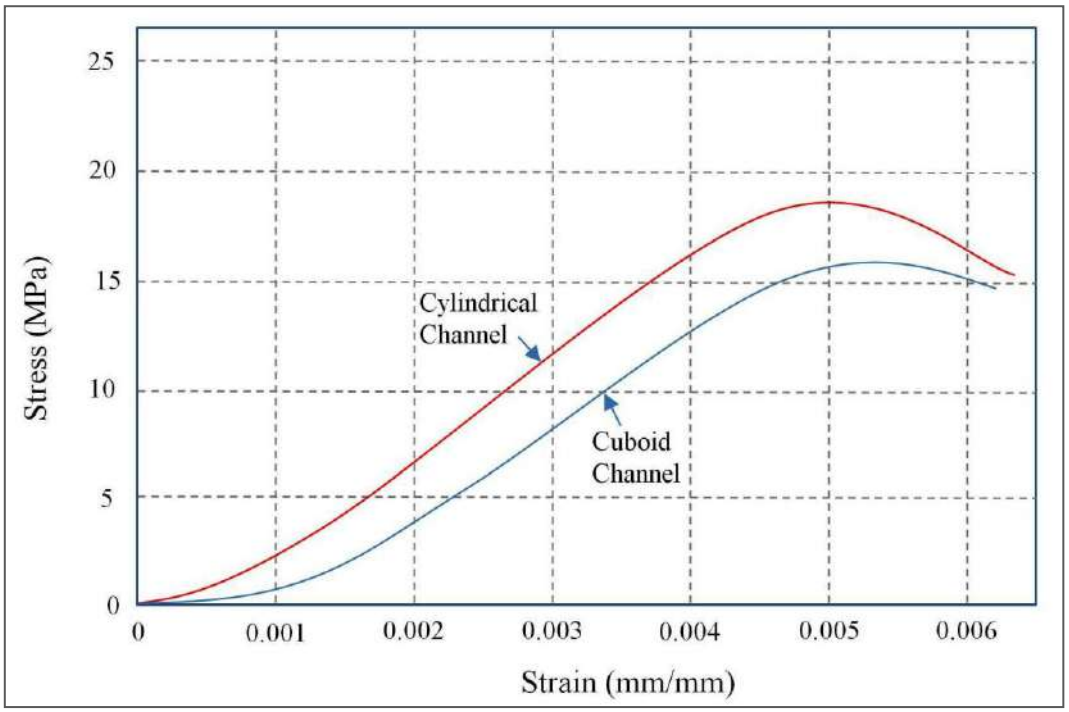

Fig. 10. - Stress-strain curves of porous scaffolds via physical testing

Conclusions

This study investigated the design, modeling, finite element analysis (FEA), and 3D printing of two distinct porous bone scaffolds, one featuring cylindrical channels and the other with cuboid channels. The CAD models for both scaffolds were created using SolidWorks® 2016 software, and their porosity was kept identical to ensure a fair comparison of their mechanical performance. The mechanical properties of the scaffolds were initially assessed using FEA in ANSYS® Workbench, where both scaffolds were subjected to a 500 N compressive load. The FEA results were carefully analyzed, focusing on total deformation, equivalent stress, and strain, which were then validated through experimental compression testing of the additively manufactured specimens. The stress-strain curves obtained from the experimental data were found to be consistent with the FEA predictions, further validating the computational approach. Notably, the scaffold with cylindrical channels exhibited superior strength under the same porosity compared to the cuboid-channel scaffold, highlighting its potential as a more robust design for bone tissue engineering applications. These findings provide valuable insights for researchers in the field, suggesting that cylindrical-channel scaffolds may offer enhanced mechanical properties.

Furthermore, this study paves the way for future research, with opportunities to explore a broader range of structural designs, varying pore shapes, porosity levels, and materials to optimize scaffolds for diverse bone regeneration applications [26-27]. From a BTE perspective, such geometrical optimization becomes particularly relevant when applied to widely used biodegradable materials such as polycaprolactone (PCL) and polylactic acid (PLA), which are extensively employed in additively manufactured scaffolds due to their biocompatibility and tunable degradation behaviour [28]. Therefore, cylindrical-channel architectures fabricated using PCL or PLA may offer improved mechanical reliability for load-bearing bone regeneration applications.

References

[1] Murr L.E. Frontiers of 3D printing/additive manufacturing: from human organs to aircraft fabrication. //Journal of Materials Science & Technology, Vol. 32, Issue 10, 2016. – p. 987-995.

[2] Salmi M. Additive manufacturing processes in medical applications. //Materials, Vol. 14, Issue 1, 2021. – p. 191.

[3] Najmon J.C., Raeisi S., Tovar A. Review of additive manufacturing technologies and applications in the aerospace industry. Additive Manufacturing for the Aerospace Industry, Elsevier, 2019. – p. 7-31.

[4] Lakhdar Y., Tuck C., Binner J., Terry A., Goodridge R. Additive manufacturing of advanced ceramic materials. //Progress in Materials Science, Vol. 116, 2021. – p. 100736.

[5] Gibson I., Rosen D., Stucker B., Khorasani M. Materials for additive manufacturing. //Additive Manufacturing Technologies, Springer Nature, Switzerland, 2021. – p. 379-428.

[6] Aslan B., Yıldız A.R. Optimum design of automobile components using lattice structures for additive manufacturing. //Materials Testing, Vol. 62, Issue 6, 2020. – p. 633-639.

[7] Tang Y., Dong G., Zhou Q., Zhao Y.F. Lattice structure design and optimization with additive manufacturing constraints. //IEEE Transactions on Automation Science and Engineering, Vol. 15, Issue 4, 2017. – p. 1546-1562.

[8] Tao W., Leu M.C. Design of lattice structure for additive manufacturing. //International Symposium on Flexible Automation (ISFA), IEEE, Cleveland, USA, 2016. – p. 325-332.
[9] Zhang Z., Joshi S. An improved slicing algorithm with efficient contour construction using STL files. //The International Journal of Advanced Manufacturing Technology, Vol. 80, 2015. – p. 1347-1362.
[10] Anastasiou A., Tsirmpas C., Rompas A., Giokas K., Koutsouris D. 3D printing: Basic concepts mathematics and technologies. //International Conference on BioInformatics and BioEngineering, IEEE, Chania, Greece, 2013. – p. 1-4.
[11] Chen S., Wang M. Fabrication, properties, and applications of scaffolds for bone tissue regeneration. //Advanced Materials Technologies, 2026. – p. e01877.
[12] Haleem A., Javaid M., Khan R.H., Suman R. 3D printing applications in bone tissue engineering. //Journal of Clinical Orthopaedics and Trauma, Vol. 11, 2020. – p. S118-S124.
[13] Lee S.S., Du X., Kim I., Ferguson S.J. Scaffolds for bone-tissue engineering. //Matter, Vol. 5, Issue 9, 2022. – p. 2722-2759.
[14] Bose S., Vahabzadeh S., Bandyopadhyay A. Bone tissue engineering using 3D printing. //Materials Today, Vol. 16, Issue 12, 2013. – p. 496-504.
[15] Sahu K.K., Modi Y.K. Investigation on dimensional accuracy, compressive strength and measured porosity of additively manufactured calcium sulphate porous bone scaffolds. //Materials Technology, Vol. 36, Issue 8, 2021. – p. 492-503.
[16] Wang C., Huang W., Zhou Y., He L., He Z., Chen Z., He X., Tian S., Liao J., Lu B., Wei Y. 3D printing of bone tissue engineering scaffolds. //Bioactive Materials, Vol. 5, Issue 1, 2020. – p. 82-91.
[17] Modi Y.K., Sahu K.K. Process parameter optimization for porosity and compressive strength of calcium sulfate based 3D printed porous bone scaffolds. //Rapid Prototyping Journal, Vol. 27, Issue 2, 2021. – p. 245-255.
[18] Gibbs D.M., Vaezi M., Yang S., Oreffo R.O. Hope versus hype: what can additive manufacturing realistically offer trauma and orthopedic surgery? //Regenerative Medicine, Vol. 9, Issue 4, 2014. – p. 535-549.
[19] Ziąbka M., Menaszek E., Tarasiuk J., Wroński S. Biocompatible nanocomposite implant with silver nanoparticles for otology – In vivo evaluation. //Nanomaterials, Vol. 8, Issue 10, 2018. – p. 764.
[20] Harper C. Handbook of Plastics, Elastomers and Composites. New York: McGraw-Hill, 2002.
[21] Elix Polymers. Products for Medical Applications. Tarragona: Elix Polymers, 2016. – Available at: http://www.elix-polymers.com (Accessed: 15/09/2025).
[22] Ziąbka M. A review of materials used in middle ear prosthetics. //Materiały Ceramiczne (Ceramic Materials), Vol. 70, Issue 1, 2018. – p. 65-85.
[23] PJ J.F., Arun K.J., Navas A.A., Joseph I. Biomedical applications of polymers – An overview. //Macromolecules, Vol. 28, Issue 4, 2018. – p. 939-944.
[24] ISO 604:2002. Plastics – Determination of Compressive Properties. Geneva: International Organization for Standardization, 2016. – Available at: https://www.iso.org/standard/31261.html (Accessed: 15/09/2025).
[25] Gorana F., Modi Y.K. Process parameter optimization for fabrication of acrylonitrile butadiene styrene parts. //Materials Today: Proceedings, Vol. 103, 2024. – p. 109-114.
[26] Gorana F., Modi Y.K. Optimization of porosity and strength of selective laser-sintered polyamide porous scaffolds useful in bone tissue engineering. //Rapid Prototyping Journal, Vol. 31, Issue 6, 2025. – p. 1141-1155.
[27] Gorana F., Modi Y.K. Multi-objective optimization for porosity and strength of selective laser sintered porous scaffolds useful in bone tissue engineering. //Iranian Journal of Science and Technology, Transactions of Mechanical Engineering, Vol. 49, Issue 3, 2025. – p. 1345-1360.

Information of the author

Modi Yashwant Kumar, PhD, Dr., associate professor, Jaypee University of Engineering and Technology
e-mail: yashwant.modi@juet.ac.in